

# Less but Better: Enabling Generalized Zero-shot Learning Towards Unseen Domains by Intrinsic Learning from Redundant LLM Semantics

Jiaqi Yue, Jiancheng Zhao, and Chunhui Zhao, *Senior Member, IEEE*

**Abstract**—Generalized zero-shot learning (GZSL) focuses on recognizing seen and unseen classes against domain shift problem where data of unseen classes may be misclassified as seen classes. However, existing GZSL is still limited to seen domains. In the current work, we pioneer cross-domain GZSL (CDGZSL) which addresses GZSL towards unseen domains. Different from existing GZSL methods which alleviate domain shift problem by generating features of unseen classes with semantics, CDGZSL needs to construct a common feature space across domains and acquire the corresponding intrinsic semantics shared among domains to transfer from seen to unseen domains. Considering the information asymmetry problem caused by redundant class semantics annotated with large language models (LLMs), we present Meta Domain Alignment Semantic Refinement (MDASR). Technically, MDASR consists of two parts: Inter-class Similarity Alignment, which eliminates the non-intrinsic semantics not shared across all domains under the guidance of inter-class feature relationships, and Unseen-class Meta Generation, which preserves intrinsic semantics to maintain connectivity between seen and unseen classes by simulating feature generation. MDASR effectively aligns the redundant semantic space with the common feature space, mitigating the information asymmetry in CDGZSL. The effectiveness of MDASR is demonstrated on the Office-Home and Mini-DomainNet, and we have shared the LLM-based semantics for these datasets as the benchmark.

**Index Terms**—Generalized zero-shot learning, unseen domain, semantic refinement, large language model, information asymmetry.

## I. INTRODUCTION

THE era of Large Language Models (LLMs) marks a tremendous leap in the ability of artificial intelligence to understand and generate natural language. With massive numbers of parameters and extensive training data (for example, GPT-3 has 175 billion parameters and 753.4 GB of training data [1]), LLMs have the capacity to internalize vast amounts of knowledge and externalize it for application in the virtual and real world [2], [3]. In some machine learning studies that fuse data and knowledge [4]–[6], researchers previously relied on the knowledge from human experts to provide models with prior information, aiming to obtain results that outperform purely data-driven techniques. The emergence of LLMs has, to some extent, supplanted the role of human experts, thereby

bringing promising prospects to data-knowledge fusion studies, such as zero-shot learning (ZSL) [7].

ZSL is designed to recognize unseen classes not present in the training set by leveraging semantic knowledge to bridge the gap between seen and unseen classes, mimicking human cognitive inference [8]–[10]. Initially, ZSL approaches like DAP [9] and ALE [11] construct mappings from data to semantics, training on seen classes and extrapolating to unseen test data, under the assumption that only unseen classes would be tested. This works well when the assumption holds, but real-world scenarios often involve a mix of seen and unseen classes. To overcome this limitation, Generalized Zero-Shot Learning (GZSL) [12]–[15] is introduced, requiring models to identify both seen and unseen classes during testing. However, ZSL models tend to misclassify unseen classes as seen due to the domain shift problem [16], [17], leading to poor GZSL performance. To combat this, generative methods such as f-CLSWGAN [13] and ABAGAN [18] have been developed, modeling between the semantic space and the feature space, generating unseen class data based on semantic knowledge to reduce model overfitting on seen classes and mitigate domain shift problem.

Before the era of LLMs, ZSL and GZSL acquired semantic knowledge through the method of expert-annotated attributes [19]. This approach is only feasible for datasets with a relatively small number of classes due to the high cost of annotation and the reliance on expert experience. For large-scale datasets, researchers often resorted to using word vectors as a means of automatically acquiring knowledge of different classes [19]. However, the semantic information contained within these vectors is not rich enough, leading to potentially suboptimal experimental results. Fortunately, as mentioned earlier, the arrival of LLMs has provided a more efficient way to acquire knowledge [20]. By crafting appropriate prompts, we can extract a vast amount of descriptive text for each class from an LLM, and the rich semantic information contained in these texts allows for the performance of ZSL at a lower cost.

Recently, the exploration of data from unseen domains and unseen classes simultaneously has garnered considerable attentions, which is called cross-domain zero-shot learning (CDZSL) [21]. The training set for CDZSL comprises data from seen classes across multiple seen domains, while the testing set consists of data from unseen classes within the unseen domain. Undoubtedly, because of the intervention of domains, CDZSL presents a greater challenge than ZSL due to its demand for a heightened level of model generalization. To address the gap of

This work was supported in part by the National Science Fund for Distinguished Young Scholars (No. 62125306) and in part by Zhejiang Key Research and Development Project (2024C01163) (*Corresponding author: Chunhui Zhao.*)

Jiaqi Yue, Jiancheng Zhao and Chunhui Zhao are with the College of Control Science and Engineering, Zhejiang University, Hangzhou, 310027, China. (Email: chhzhaoc@zju.edu.cn)

unseen classes and domains, Mancini et al. employed the Mixup technique [22] and introduced CuMix [21]. This approach utilizes the underlying structure of ZSL methods, mapping data to the feature space before subsequently mapping features to the semantic space. During the training process, samples from diverse domains and classes are intermixed within the data and feature spaces, effectively simulating novel domains and classes. Building upon CuMix, SEIC [23] introduced intermediate classes to imbue the feature embedding space with semantic meaning. The semantic knowledge utilized by these methods is still in the form of word vectors.

Just like in ZSL, CDZSL also makes an assumption about the inference process: during the testing phase, only unseen classes from unseen domains are present. We believe that the assumption of CDZSL does not agree well with reality, as in real-world scenarios, both seen and unseen classes are likely to occur. Hence, we first introduce Cross-Domain Generalized Zero-Shot Learning (CDGZSL) and demonstrate it in Fig. 1. In CDGZSL, the training set includes seen class data from multiple seen domains, while the test set includes both seen and unseen class data from the unseen domain. A comparison between zero-shot learning, generalized zero-shot learning, cross-domain zero-shot learning, and cross-domain generalized zero-shot learning can be seen in Table I. Existing studies encompass zero-shot learning, generalized zero-shot learning and cross-domain zero-shot learning. Generalized zero-shot learning removes the inference assumption of zero-shot learning but maintains the assumption of the single domain. In contrast, cross-domain zero-shot learning, despite its ability to handle multiple domains, does not eliminate the inference assumption. This demonstrates that generalized zero-shot learning and cross-domain zero-shot learning both have assumptions, and cross-domain generalized zero-shot learning breaks the limitations of both, resulting in test scenarios that agree well with reality.

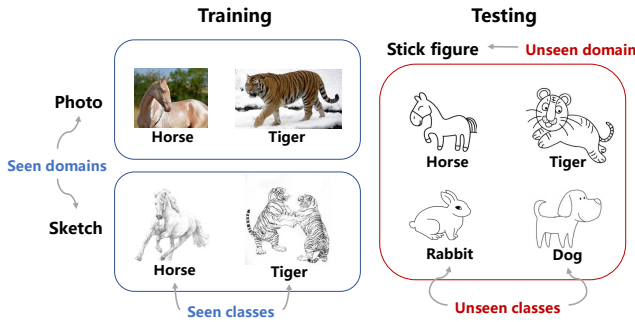


Fig. 1. The setting of CDGZSL. The training set includes seen classes in seen domains, and the testing set includes both seen and unseen classes in unseen domains.

Although generative methods could be employed to address the transition from zero-shot learning to generalized zero-shot learning, the same approach cannot be directly applied from cross-domain zero-shot learning to cross-domain generalized zero-shot learning. For the sake of cost-effectiveness and speed, a large volume of class description text can be obtained from LLMs as semantics, and is applied to all domains (including seen and unseen domains). However, this leads

TABLE I  
COMPARISON AMONG SEVERAL ZSL SETTINGS.

Setting	Existing Research	Domain	Inference Class	Assumption
ZSL	✓	Single	Unseen class only	✓
GZSL	✓	Single	Seen & unseen class	✓
CDZSL	✓	Multiple	Unseen class only	✓
CDGZSL	✗	Multiple	Seen & unseen class	✗

\* ✓ indicates the presence of research or assumption, while ✗ represents the opposite meaning.

to the asymmetry between the low information density of semantic modality and the high information density of feature modality. In terms of the semantic modality, a significant portion of the large-volume LLM semantics is not intrinsic semantics which are shared across domains, leading to a low knowledge information density. For the feature modality, in order to generalize from seen domains to unseen domains, the generator needs to produce features within a common feature space shared by all domains. However, this common feature space encapsulates the essence of each class and thus has a higher information density. This asymmetry poses a challenge for the generator to accurately model the relationship between these two modalities. It results in greater differences between the generated features for unseen classes and their actual features, making it difficult to address the domain shift problem when transitioning from CDZSL to CDGZSL.

In this paper, we introduce a novel approach named Meta Domain Alignment Semantic Refinement (MDASR) aimed at enabling GZSL towards unseen domains. To address the aforementioned issue of information asymmetry, unlike existing ZSL, GZSL and CDZSL endeavors, we learn intrinsic information from the redundant semantics and perform generative modeling between the refined semantics and domain common features, which are symmetrical in information density, to mitigate the domain shift problem. To this end, MDASR includes two optimization objectives: Inter-class Similarity Alignment (ISA) and Unseen-class Meta Generation (UMG). Guided by the feature space, ISA eliminates non-intrinsic semantics while UMG preserves intrinsic semantics. Specifically, on the one hand, ISA leverages the fundamental and invariant relationships between classes, which are derived from multi-domain data, as a standard to remove non-intrinsic semantics. On the other hand, UMG simulates the generation process of unseen class features to ensure the semantic linkage from seen to unseen classes remains unbroken, thus preserving intrinsic semantics. In summary, our method, through ISA and UMG, addresses the issue of information asymmetry between semantic and feature spaces, thereby alleviating the domain shift problem in CDGZSL. The total contributions of this paper are summarized below.

- 1) We have introduced CDGZSL firstly, overcoming the inability of CDZSL towards unseen domains to recognize seen and unseen classes. Furthermore, we have uncovered the bottleneck of CDGZSL, i.e., information asymmetry

caused by semantic redundancy, and addressed it from the perspective of intrinsic semantic learning.

- 2) A novel MDASR framework is designed to eliminate non-intrinsic semantics and preserve intrinsic semantics through ISA and UMG. This method refines the low-information-density semantic space under the guidance of the high-information-density feature space.
- 3) We first verify the CDGZSL capability of MDASR on two open-source datasets, Office-Home and Mini-DomainNet, and we have made the corresponding LLM-based semantic texts for these datasets available to the public, providing a benchmark for subsequent researchers.

## II. MOTIVATION

In this section, we would like to clarify our motivation: the problem of semantic variation and redundancy, and the resulting information asymmetry between semantic space and feature space that makes the solving of domain shift problem in CDGZSL more difficult.

### A. The problem of semantic variation and redundancy

We would like to introduce the semantic variation caused by multiple domains, as well as the issue of redundancy arising from the general semantic descriptions.

1) *Semantic variation*: Data from multiple domains represent different manifestations of the same class, resulting in semantics that are valid in a specific domain often being invalid in different domains. We demonstrate this concept in Fig. 2 by leveraging a simple example. When describing an orange cat, the following semantics could be given: orange, with hair, and with a tale. In the domain of photos, these semantics are all valid. However, in the domain of sketches, the color-related semantic ‘orange’ becomes invalid. Moreover, the texture-related semantic ‘with hair’ is not applicable as well in the domain of stick figures. This indicates that the semantics associated with a class can vary as the domain changes.

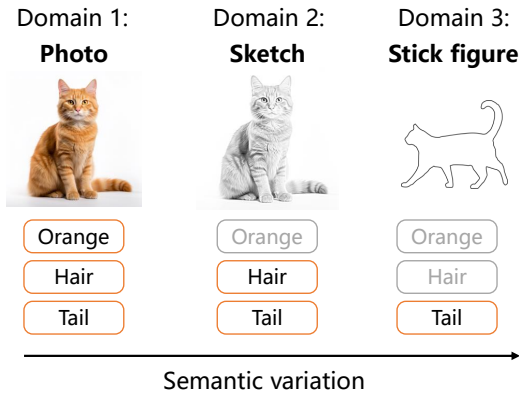


Fig. 2. An example of semantic variation.

2) *Semantic redundancy*: To capture the semantics of a class, we could employ LLMs for their comprehensive descriptions. The semantic descriptions labeled by LLMs are usually extensive texts containing general information about

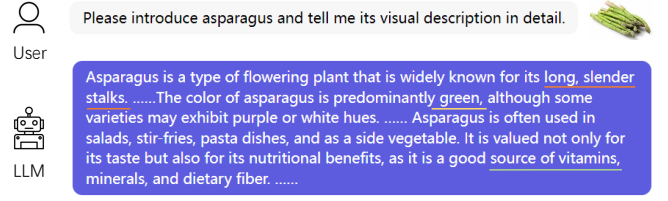


Fig. 3. Demonstration of the redundancy in semantic annotations by LLMs. The orange line represents intrinsic semantics, the yellow line may disappear due to domain influence, and the green line is completely unrelated to vision.

the object. However, this also leads to a lot of redundant information. We provide an example in Fig. 3, where we asked the LLM to provide the semantics of asparagus. The semantics provided include shape, color, and nutrition. Shape generally remains unchanged and is the intrinsic semantic; color may become redundant with changes in domain; nutrition is unrelated to visual features and is definitively redundant information.

As shown in Fig. 4, for the large volume of semantics provided by LLMs (represented by the light blue bar), only a part of the semantics are intrinsic (represented by the dark blue bar) because they are the intersection of effective semantics across various domains. Therefore, although LLMs can provide comprehensive descriptions, they are less effective for cross-domain transfer because they fail to capture the intrinsic semantics.

**Remark:** In the present CDZSL and our CDGZSL, general class descriptions are obtained and applied directly to all domains, thereby resulting in the above semantic redundancy. Precise class descriptions for each domain still demand extensive expert review and thus are beyond our current scope.

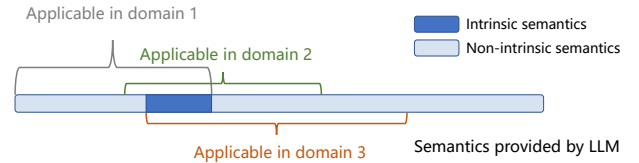


Fig. 4. The redundancy of LLM semantics. Only a part of semantics is shared across domains.

### B. Information asymmetry between semantics and features

If we would like to address domain shift problem, a generator is needed to model the relationship between the modalities of semantics and features and generate features of unseen classes [24]. However, there is an information asymmetry between the two modalities, as shown in Fig. 5, impeding the effectiveness of generative methods in transitioning from CDZSL to CDGZSL.

The information asymmetry between the semantic and feature modalities originates from their different information densities. In this paper, information density is defined as the proportion of shared information across domains relative to all information.

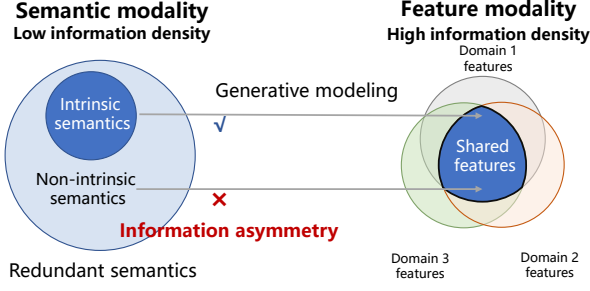


Fig. 5. The information asymmetry between semantic and feature modality. The non-intrinsic semantics have no corresponding part in the shared features.

For the semantic modality, the intrinsic semantics shared by each domain only account for a portion of the general semantics provided by the LLM, while the rest of the information is non-intrinsic, resulting in low information density, as shown in the left half of Fig. 5. In contrast, for the feature modality, existing transfer learning methods can extract the common feature space across domains, eliminating domain-specific information, thus leading to high information density, as represented by the dark blue overlapping area in the right half of Fig. 5.

In fact, the solution lies in obtaining the common features and identifying the corresponding intrinsic information within the semantics. The prior problem has been resolved by predecessors, making it simpler, whereas the latter remains unsolved, presenting more of a challenge. If the information asymmetry is not tackled, the generator could only be trained with non-intrinsic semantics mixed together, which harms the address of domain shift problem.

### III. METHODOLOGY

In this section, we first introduce the problem formulation and notations used in this paper. From there, the process of utilizing LLMs for extracting semantics of various classes is explored. This is followed by a recapitulative explanation of the proposed MDASR. Then, the detailed paradigm for visual alignment and meta semantic refinement is presented. We end the section with the CDGZSL inference procedure.

#### A. Problem formulation and notations

In the task of CDGZSL, our goal is to recognize both seen and unseen classes in the unseen domain. Only labeled seen class samples from multiple seen domains and their corresponding semantics are provided during training.

Formally, let  $\mathcal{X}$  denote the input space (such as the image space),  $\mathcal{A}$  denote the semantic space (such as the text or attribute space),  $\mathcal{Y}$  the set of possible classes, and  $\mathcal{D}$  the set of possible domains. In the training stage, a set  $\mathcal{S} = (x_i, y_i, a_i, d_i)_{i=1}^n$  is given, where  $x_i \in \mathcal{X}$ ,  $y_i \in \mathcal{Y}^s$ ,  $a_i \in \mathcal{A}^s$ , and  $d_i \in \mathcal{D}^s$ . Note that  $\mathcal{Y}^s$  and  $\mathcal{A}^s$  are the labels and semantic space of seen classes, respectively, and  $\mathcal{Y}^s \in \mathcal{Y}$ ,  $\mathcal{A}^s \in \mathcal{A}$ .  $\mathcal{D}^s$  is the set of seen domains, including  $K$  seen domains ( $K \geq 2$ ), and  $\mathcal{D}^s \in \mathcal{D}$ .

Given  $\mathcal{S}$ , we aim at learning a function mapping an image  $x$  of unseen domains  $\mathcal{D}^u \in \mathcal{D}$  to its corresponding label in

a set of classes  $\mathcal{Y}$ .  $\mathcal{D}^s \cap \mathcal{D}^u = \emptyset$ . Following the setting of GZSL,  $\mathcal{Y} = \mathcal{Y}^s \cup \mathcal{Y}^u$ , where  $\mathcal{Y}^u$  are the labels space of unseen classes, and  $\mathcal{Y}^s \cap \mathcal{Y}^u = \emptyset$ . Note that during testing,  $\mathcal{A}^u$  are provided, which is the semantic space of unseen classes.

#### B. Extracting semantics via LLMs with prompt engineering

In this subsection, we outline how to obtain the semantics of various classes through LLMs. We define a prompt  $P$ , and for a given class  $y_i$ , by embedding  $y$  into  $P$ , we form the input to LLMs. Consequently, the output text of the LLMs can serve as the semantic representation of that class. Mathematically, this can be expressed as  $A_i = LLM(P(y_i))$ . Next, we will introduce the construction of  $P$  used in this study.

We leverage a one-shot learning approach with our prompt to obtain a comprehensive semantic description from an LLM. We construct an example within the LLM input, which guides the LLM in learning the example’s characteristics and generating the required semantics. Our prompt encompasses three key components: the class  $y_i$  to be queried, a demonstrative class, and the description text of the demonstrative class. The structure is as follows: “Please provide a detailed visual feature description for the class  $\{y_i\}$ . For your reference in answering, consider the visual feature description given for the  $\{\text{Eiffel Tower}\}$  as follows: {a reliable and rich description text about the Eiffel Tower excerpted from Wikipedia}.” In this prompt, the Eiffel Tower serves as the demonstrative class, and the model will adjust the style of the output semantics based on the descriptive text of the demonstrative class, thus making the acquisition of semantics more controllable.

#### C. Overall framework of MDASR

In this section, we provide a comprehensive overview of the proposed Meta Domain Alignment Semantic Refinement (MDASR), as depicted in Fig. 6. The process begins with training samples of multiple seen domains, from which we train a data encoder which aligns different domains, denoted as  $E_d$ , to construct a common feature space,  $\Psi$ . This space encapsulates the shared and distinguishable features across the seen domains, thus offering high generalizability to the unseen domain.

To achieve CDGZSL in  $\Psi$ , we need to generate reliable features of unseen classes based on their semantics. As discussed in Section II, it is crucial to obtain the intrinsic semantics to mitigate the issues of semantic redundancy. Consequently, we introduce a meta semantic refinement framework designed to optimize the semantic encoder  $E_s$ , guided by features within  $\Psi$ . This approach preserves valuable semantic information for future feature generation. Finally, by utilizing the generated unseen features in conjunction with real seen features, we can facilitate cross-domain generalized zero-shot classification of samples from unseen domains.

#### D. Adversarial construction of common feature space

To construct the common feature space across different domains, we employ the Domain-Adversarial Neural Network technique [25]. For this part, specifically refer to the upper



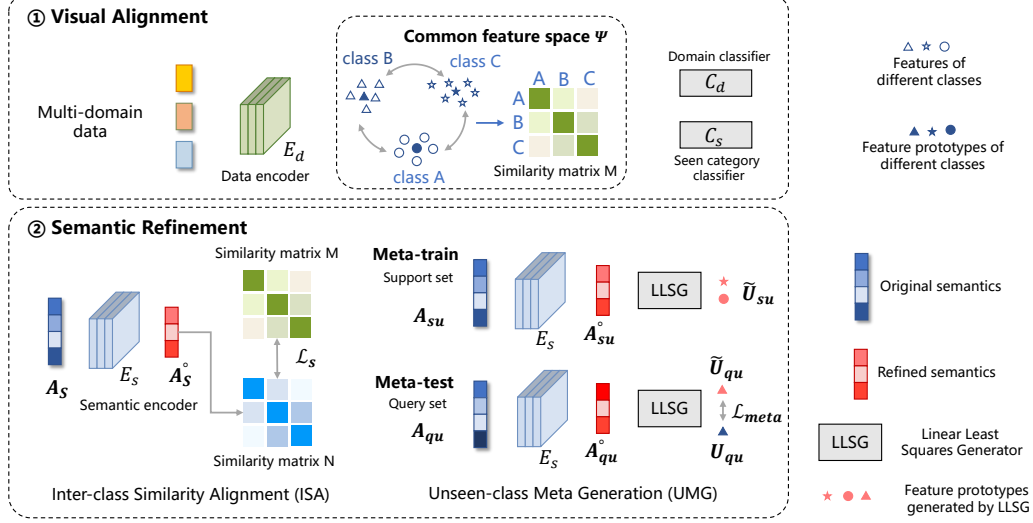


Fig. 6. The framework of proposed Meta Domain Alignment Semantic Refinement (MDASR).

half of Fig. 6. We establish three networks: the data encoder  $E_d$ , the domain classifier  $C_d$ , and the seen-class classifier  $C_s$ , parameterized by  $\theta$ ,  $\mu$ , and  $\sigma$  respectively. It should be noted that only training data from seen classes in the seen domains is provided.

In particular, the data encoder  $E_d$  maps data from various seen domains into the feature space, subsequently engaging in a min-max game with the domain classifier  $C_d$ . The role of  $C_d$  is to discern the domain of different features, while  $E_d$  modifies the feature space to confuse  $C_d$ . Concurrently, the seen-class classifier  $C_s$  ensures that the features remain classifiable. The loss functions of  $C_d$  and  $C_s$  can be represented as follows:

$$\mathcal{L}_d = - \sum_{i=1}^k 1[y_i^d] \log(C_d(E_d(x_i))) \quad (1)$$

$$\mathcal{L}_c = - \sum_{i=1}^k 1[y_i^c] \log(C_s(E_d(x_i))) \quad (2)$$

Here,  $x_i$  denotes the  $i$ -th training sample,  $k$  the total number of training samples, and  $y_i^d$  and  $y_i^c$  represent the domain and class labels of  $x_i$  respectively.  $1[\cdot]$  serves as the indicator function.

Consequently, the total training objective of the data encoder  $E_d$  can be expressed as:

$$\min_{\sigma, \theta} \max_{\mu} \frac{1}{k} \mathcal{L}_c - \frac{\lambda}{k} \mathcal{L}_d \quad (3)$$

where  $\lambda$  is a trade-off coefficient. We designate the feature space generated by the data encoder  $E_d$  as  $\Psi$ , housing the shared features of the seen domains.

#### E. Meta semantic refinement in common space

As emphasized in the motivation, if the semantic redundancy cannot be eliminated, the resulting information asymmetry

would reduce the quality of the generated features for unseen classes. Therefore, in this subsection, we propose a meta semantic refined method, which includes two parts: The first part is inter-class similarity alignment, which can eliminate non-intrinsic semantics that could fail due to domain changes, but it may also inadvertently remove intrinsic information. The second part is unseen-class meta generation, which protects the intrinsic semantic information from being eliminated and maintains the ability of refined semantics to connect seen and unseen classes.

1) *Inter-class similarity alignment (ISA)*: Due to the presence of non-intrinsic semantics, the inter-class similarity obtained directly from the original semantics differs from the inter-class similarity obtained in the data-driven feature space  $\Psi$ . Therefore, if we can refine the semantics based on the generalizable inter-class similarity in the common space  $\Psi$ , we can indirectly remove the non-intrinsic semantics. Specifically, we construct the inter-class similarity leveraging the dark knowledge contained in the output of classifier  $C_s$ . The reason for using dark knowledge is that studies have shown that irrelevant information, like background details, still persists in the feature space [26]. In contrast, dark knowledge, found in the classifier's final layer, could better represent the essential information in the feature space related to class semantics because it bases the perspective of the final classification. Therefore, we can leverage the class similarity relationships calculated by dark knowledge and the similarity relationships calculated by semantics to establish the refinement constraint. The content of this part is displayed in the lower left corner of Fig. 6.

First, we come to the dark knowledge similarity part. Specifically, we obtain the dark knowledge in the form of logits. Logits are the raw, unnormalized outputs of a softmax classifier that represent the model's predicted log-odds for each class before being transformed into probabilities by the softmax

function. We compute the average dark knowledge for the  $t$ -th seen class  $P_t$  as:

$$P_t = \frac{1}{n_t} \sum_{i=1}^{n_t} C'_s(E_d(x_i^t)) \quad (4)$$

where  $C'_s$  represents the logits of  $C_s$  passed through a softmax with a temperature coefficient of  $T$ , and  $n_t$  is the number of samples for the  $t$ -th seen class. This can be considered as a kind of embedding of the class.

Subsequently, the seen-class similarity matrix  $M$  in the common feature space  $\Psi$  can be calculated as:

$$M(i, j) = \cos(P_i, P_j) \quad (5)$$

$\cos$  represents the cosine similarity, and  $M$  represents the similarity of each class dark knowledge prototype in  $\Psi$ .

Next, we come to the semantic similarity part. We build a semantic encoder  $E_s$  for semantic refinement. It should be noted that our approach is applicable to different kinds of semantics. If the semantics are text extracted from LLMs, the initial  $E_s$  could be a pre-trained sentence-Bert [27] that maps a paragraph to a fixed-length vector. If the semantics are attributes provided by human experts,  $E_s$  could be a multi-layer perceptron network. With the semantic encoder  $E_s$ , the refined semantics can be expressed as:

$$A^\circ = E_s(A) \quad (6)$$

Based on this, we can also obtain the similarity matrix  $N$  of refined semantics  $A^\circ$ :

$$N(i, j) = \cos(A_i^\circ, A_j^\circ) \quad (7)$$

$A_i^\circ$  and  $A_j^\circ$  represent the refined semantics of the  $i$ -th seen class and the  $j$ -th seen class, respectively.

After the non-intrinsic semantics are eliminated, the inter-class similarity of semantics will become closer to the similarity in the feature space, because the common feature space does not include non-intrinsic semantic information. Therefore, if  $M$  and  $N$  are closely aligned, the semantic redundancy could be mitigated. The related loss function could be expressed as:

$$\mathcal{L}_s = \|M - N\| \quad (8)$$

2) *Unseen-class meta generation (UMG)*: Refining semantics solely at the level of inter-class similarity is not enough, because it could result in the loss of intrinsic information that connects seen to unseen classes. In other words, it is necessary to ensure that the intrinsic semantics are preserved and generators trained with the refined semantics can synthesize fake unseen features that are minimally different from the real ones. However, since the real unseen features are inaccessible during the training phase, guaranteeing the above condition is challenging. To address this challenge, we can simulate this process within the training set to ensure the preservation of intrinsic semantics.

In order to simulate the ZSL generation process, we implement our semantic refinement within the meta-learning framework. The content of this part is displayed in the lower

right corner of Fig. 6. Differing from traditional machine learning, the fundamental unit of meta-learning is a task, not a sample. For each task  $\mathcal{T}_i = \{\mathcal{T}_{su}, \mathcal{T}_{qu}\}$ , drawn from the task distribution  $p(\mathcal{T})$ , the support set  $\mathcal{T}_{su}$  comprises  $N_{su}$  seen classes, while the query set  $\mathcal{T}_{qu}$  includes  $N_{qu}$  seen classes. To mirror the ZSL process, the classes within the support set and the query set are disjoint. Generators that fit the features of support classes with the semantics refined by  $E_s$  should be capable of generating reliable features of query classes. For each pair of support and query sets, we can generate the refined support set semantics using  $E_s$ , and then fit the support set and validate it with the query set for these respective tasks. Therefore, we could employ the loss to optimize semantic encoder  $E_s$  to ensure it preserve intrinsic semantics beneficial to generation.

Specifically, within each task, we utilize  $E_s$  to obtain refined support set semantics  $A_{su}^\circ$  and then train a generator from support classes. After that, fake query features are synthesized by refined query semantics and the above generator. Since real query features are at hand, loss of the query set could be calculated. We employ the loss of each task's query set to evaluate the effectiveness of  $E_s$ . If the loss on each task is relatively small, this indicates that the current  $E_s$  is near optimality. Otherwise, we could optimize  $E_s$  using the gradient of this loss with respect to  $E_s$ . In order to make the loss of the query set have an effective gradient with respect to  $E_s$ , a linear least squares generator (LLSG)  $z$  is leveraged here, where the independent variable is refined class semantics and the dependent variable is the prototype of class features, as only a linear generator can obtain the following analytic solution:

$$U_{su} = A_{su}^\circ z + \xi \quad (9)$$

$$z^* = (A_{su}^\circ)^+ U_{su} \quad (10)$$

$$(A_{su}^\circ)^+ = ((A_{su}^\circ)^T A_{su}^\circ + \alpha I)^{-1} (A_{su}^\circ)^T \quad (11)$$

where  $U_{su}$  is the prototypes of support class features (which are their centers),  $\xi$  is the residual error,  $(A_{su}^\circ)^+$  is the pseudo-inverse of  $A_{su}^\circ$ , and the solution of  $z$  is  $z^*$ .  $\alpha$  is a small number to ensure the success of the inversion.

The fake query feature prototypes  $\tilde{U}_{qu}$  produced by  $z^*$  could be presented as:

$$\tilde{U}_{qu} = E_s(A_{qu}) z^* \quad (12)$$

Therefore, the loss of the query set can be calculated as follows:

$$\mathcal{L}_q = \|U_{qu} - \tilde{U}_{qu}\| \quad (13)$$

It's easy to find (13) is only differential to the parameter of  $E_s$ , and the meta-loss can be obtained from each task and optimize  $E_s$ .

$$\mathcal{L}_{meta} = \frac{1}{n_T} \sum \mathcal{L}_q \quad (14)$$

where  $n_T$  is the number of sampled tasks.

Considering the similarity constraint, the final loss of meta semantic refinement could be represented as:

$$\mathcal{L}_{total} = \mathcal{L}_{meta} + \mathcal{L}_s \quad (15)$$

With the optimized  $E_s$ , we could obtain the refined semantics  $A^\circ$ , including the seen and unseen classes, which are  $A_s^\circ = E_s(A_s)$  and  $A_u^\circ = E_s(A_u)$ .

3) *Feature generation with refined semantics*: In this stage, we would like to train a formal generator that can synthesize features in the common space under the condition of  $A^\circ$ . Then, the fake unseen features and real seen features are leveraged together to obtain the final classifier. Specifically, we utilized WGAN-GP [28] as our formal generator and the training process is shown as follows:

$$\mathcal{L}_{WGAN-GP} = E[D(f)] - E[D(\tilde{f})] - \beta E[\|\nabla_{\tilde{f}} D(\tilde{f})\|_2 - 1]^2 \quad (16)$$

$$\min_G \max_D \mathcal{L}_{WGAN-GP} \quad (17)$$

where  $E$  represents the empirical expectation,  $G$  and  $D$  represent the generator and discriminator of WGAN-GP,  $f$  represents the real features, and  $\tilde{f}$  represents the generated features,  $\beta$  is a hyperparameter.

The generator is trained on seen class data conditioned on the refined semantics  $A^\circ$ . Because of the refined semantics, the information asymmetry between semantic space and feature space is solved beforehand, and this decreases the difficulty of the mapping of the generator.

After training the generator, we could obtain the fake unseen features through:

$$\tilde{f}_u = G(A_u^\circ, \epsilon) \quad (18)$$

where  $\epsilon$  is the random sampled Gaussian noise.

Combining the real seen features and the fake unseen features, the CDGZSL classifier could be trained.

$$C_c = MLP(\tilde{f}_u, f_s) \quad (19)$$

where  $MLP$  is a multi-layer perceptron net.

#### F. The CDGZSL inference procedure

In the last subsection, we would like to introduce the inference process of MDASR. For testing data  $x_t$ , which comes from the unseen domain and could belong to seen and unseen classes, we first map it to the common feature space with data encoder  $E_d$ , and then predict its label with CDGZSL classifier  $C_c$ . The whole process could be formalized as follows:

$$\hat{y} = C_c(E_d(x_t)) \quad (20)$$

Because  $C_c$  is trained by both real seen features and fake unseen features with less effect of semantic redundancy, the domain shift problem could be further alleviated, and we could gain a more accurate classifier of CDGZSL.

### IV. EXPERIMENT

In this section, we have verified the proposed MDASR on two public datasets, Office-Home [29] and Mini-DomainNet [30]. At the same time, we have also carried out a series of comparative experiments, and ablation studies to further demonstrate the effectiveness of the proposed method.

#### A. Datasets and relative semantics

Different from the existing CDZSL studies which utilize word vector [31] to serve as semantics, we employ LLMs to extract semantics for the two datasets. In this way, we could validate the performance of our proposed methodology in refining LLM semantics. Due to the relatively small number of categories in Office-Home, in addition to LLM semantics, we also provide a manually annotated class-attribute matrix, which is the traditional form of semantics for ZSL, used for comparison with the semantics provided by LLM. For the convenience of other researchers, we provide all the above semantics on the Internet.<sup>1</sup>

1) *Office-Home*: The Office-Home dataset is a popular dataset used for multi-domain transfer learning tasks. It contains about 15,500 images that belong to 65 different object classes. The images are sourced from four significantly different domains: *Art*, *Clipart*, *Product*, and *Real-world*. As mentioned earlier, in the semantic annotations of the Office-Home dataset, we employed two forms: LLM annotation and manual annotation. For LLM annotation, as mentioned in Section III.B, we employed GPT-3.5 [32] as the LLM to obtain descriptive paragraphs as semantics for each class. For manual annotation, we first predefined 21 attributes, including the material, size, color, etc., and annotated the 65 classes, forming a  $65 \times 21$  class-attribute matrix, with elements being 0 or 1.

2) *Mini-DomainNet*: The Mini-DomainNet is a large-scale dataset which simplified from the DomainNet [33] dataset. It contains about 140000 images that belong to 126 different object classes. The images are sourced from four diverse domains: *Art*, *Clipart*, *Sketch*, and *Real*. Compared to Office-Home, Mini-DomainNet has more classes, consumes more computational resources, and poses greater challenges. Due to the large number of classes in this dataset, we did not have the resources to perform manual annotations, so we only employed the LLM for semantic annotation.

#### B. Experimental details

In CDGZSL, there are both seen and unseen domains, as well as seen and unseen classes. For Office-Home, the allocation of seen and unseen domains is as follows: *Art*, *Clipart*, and *Product* are each designated as the unseen domain in turn. When a domain is designated as the unseen domain, the other three domains serve as the seen domains. Because we employ Resnet-50 pretrained on Imagenet [34] as the initial parameters for the data encoder  $E_d$ , only the *Real-world* domain is not used as the unseen domain (since it is more similar to Imagenet) among these four domains. Additionally, the division of seen and unseen classes is as follows: we select 5 classes that do not appear in Imagenet as unseen classes, 5 classes as validation, and the remaining 55 classes as seen classes. For Mini-DomainNet, similarly, aside from the *Real* domain, the other three domains each take a turn as the unseen domain once. Also, we select 13 classes that do not appear in Imagenet as unseen classes, 13 classes as validation, and the remaining classes as seen classes.

<sup>1</sup><https://github.com/chunhuiZ/Semantics-of-OfficeHome-and-MiniDomainNet>

TABLE II  
THE CDGZSL RESULTS ON OFFICE-HOME DATASET

Semantics	Methods		Art			Clipart			Product		
			S	U	H	S	U	H	S	U	H
LLM text	CuMix	img-only	59.43	0	0	50.91	3.28	6.16	66.21	0.72	1.42
		two-level	57.37	1.85	3.58	50.77	3.61	6.74	66.88	0.70	1.38
		original	57.83	2.46	4.71	51.19	3.94	7.31	65.09	1.80	3.50
	S-AGG		55.09	1.23	2.40	49.90	7.56	13.13	63.38	2.52	4.84
	SEIC		56.64	2.48	4.75	48.49	8.55	14.53	63.19	3.97	7.47
	f-CLSWGAN	original	56.90	43.15	49.08	53.56	28.26	36.99	72.94	34.46	46.80
		PCA	57.50	38.88	46.39	53.53	25.98	34.98	73.61	27.07	39.58
	MDASR		55.10	50.62	<b>52.76</b>	52.67	36.18	<b>42.89</b>	73.19	38.26	<b>50.25</b>
Attribute	CuMix	img-only	43.81	4.93	8.86	41.10	2.96	5.52	56.49	2.52	4.82
		two-level	43.45	5.56	9.85	39.35	4.60	8.23	55.17	6.49	11.61
		original	44.28	6.17	10.83	38.95	7.23	12.19	53.16	9.38	15.94
	S-AGG		45.31	5.60	9.96	37.23	8.89	14.35	50.41	7.94	13.71
	SEIC		43.50	6.27	10.96	41.41	5.26	9.33	54.70	6.85	12.17
	f-CLSWGAN	original	54.85	35.18	42.87	53.42	28.94	37.54	72.91	32.12	44.59
		PCA	57.85	31.48	40.77	53.92	29.29	37.95	72.94	22.02	33.82
	MDASR		59.10	38.27	<b>46.45</b>	53.28	30.26	<b>38.60</b>	72.99	40.07	<b>51.74</b>

\* The bold values represent the highest H-accuracy in each part.

For the various networks used in the experiments, the specific details are as follows: The data encoder  $E_d$  is the encoder of Resnet50, with initial parameters trained on Imagenet; The domain classifier  $C_d$ , seen class classifier  $C_s$ , and the final CDGZSL classifier  $C_c$  are all single-layer fully connected layers followed by Softmax. The semantic encoder  $E_s$  is divided into two cases: When the semantics are text generated by LLM,  $E_s$  is sentence-Bert [27], with initial parameters using all-MiniLM-L6-v2, and only the last two layers are fine-tuned during training. When the semantics are manually annotated attributes,  $E_s$  is a two-layer fully connected layer with an output dimension of 15. The generator and discriminator of WGAN-GP are also both two-layer fully connected layers. The activation function of all the above-mentioned fully connected layers is ReLU. For the optimizers and various hyperparameters used in training, the specific details are as follows:  $\lambda = 1$ ,  $T = 5$ ,  $\alpha = 0.1$ ,  $\beta = 1$ , the optimizer is Adam, and the learning rate is  $2 \times 10^{-4}$ .

For the accuracy metric, we adopt three indicators: Seen class accuracy S, which is the ratio of seen class samples in the unseen domain being correctly classified; Unseen class accuracy U, which is the ratio of unseen class samples in the unseen domain being correctly classified; H-accuracy, the harmonic mean of S and U, i.e.,  $H = 2SU/(S+U)$ . Consistent with previous GZSL work, among these, the one that best reflects the performance of the CDGZSL algorithm is the H-accuracy.

### C. Results on Office-home and Mini-DomainNet

We have adopted six comparative methods to compare with the proposed MDASR. Specifically, these six methods can

be divided into CDZSL methods (including CuMix [21] and its two variants (img-only and two-level), S-AGG [35], and SEIC [23]) and generative method modified to apply in various domains (f-CLSWGAN [13]). CDZSL methods encompass the current approaches that aim to identify unseen classes in unseen domains. However, due to the influence of the domain shift problem, they are not very effective at recognizing both seen and unseen classes simultaneously. Comparatively, generative methods can better overcome the impact of domain shift problem, but it is not designed for CDGZSL. These comparative methods utilize semantics in two ways: when semantics exist in the form of an attribute matrix, they can be used directly; when semantics are in text form, they can first be converted into sentence vectors using sentence-Bert, and then utilized. Since our proposed method is a generative approach with meta semantic refinement, we also employed PCA [36] as another semantic refinement method for comparison.

For the Office-home dataset, we utilized two types of semantic sources: one acquired from querying LLMs and the other manually annotated. The results for both types of semantics are displayed in Table II. It is evident that the proposed MDASR outperforms other methods with both LLM-provided semantics and manually annotated semantics, with the former even surpassing the performance of the latter. We believe this is because the Office-home dataset consists of everyday items, which LLM is already capable of describing comprehensively, whereas manually provided semantics are limited by the annotators' energy and ability to provide a thorough description. However, expert intervention may still be necessary in some non-daily scenarios like industry and medicine. Observing the comparative methods, the existing four CDZSL methods, CuMix and its variants ("img-only" and



TABLE III  
THE CDGZSL RESULTS ON MINI-DOMAINNET DATASET

Methods		Clipart			Painting			Sketch		
		S	U	H	S	U	H	S	U	H
CuMix	img-only	63.98	2.67	5.12	63.69	2.64	5.06	59.61	1.86	3.60
	two-level	64.54	3.32	6.31	64.20	2.58	4.96	59.75	3.42	6.46
	original	64.20	2.49	4.79	64.27	3.10	5.91	54.70	5.07	9.27
S-AGG		63.98	2.89	5.53	62.65	0.90	1.77	56.96	1.91	3.69
SEIC		64.24	2.01	3.89	63.46	1.09	2.14	58.45	1.08	2.12
f-CLSWGAN	original	61.38	24.53	35.05	58.23	23.31	33.29	56.60	22.03	31.71
	PCA	64.51	22.27	33.10	66.73	11.10	19.03	58.79	8.62	15.03
MDASR		63.69	29.43	<b>40.25</b>	61.02	26.16	<b>36.62</b>	55.16	28.25	<b>37.36</b>

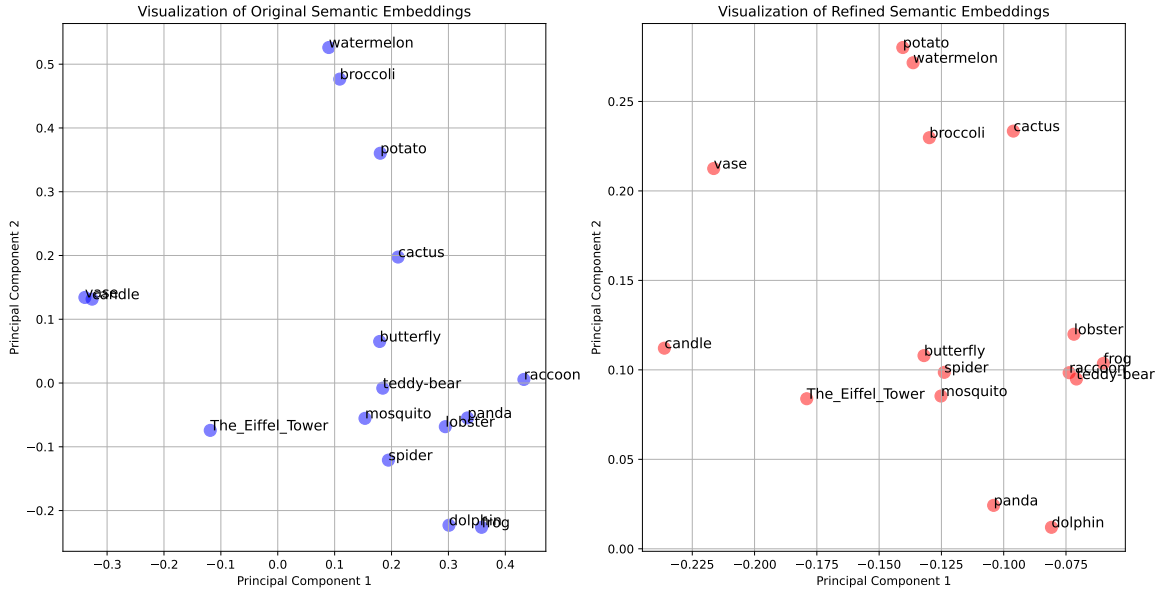


Fig. 7. Visual comparison between the original semantic embeddings and the semantic embeddings refined by MDASR.

“two-level” respectively refer to performing mixup only in the image space and performing mixup in both the image and feature spaces), S-AGG, and SEIC, all have a lower accuracy for unseen classes due to domain shift problem. In comparison, generative methods can somewhat overcome this issue. It can be observed that the modified f-CLSWGAN is the current state-of-the-art. Meanwhile, the PCA semantic refinement used for comparison has negative effects on generative methods most time. The performance can often tend towards degradation. This is because the optimization of PCA does not consider the effect of semantic redundancy, and does not take measurement to preserve effective semantics. The proposed MDASR, in contrast, enhances performance over f-CLSWGAN across different semantics and domains.

For the Mini-DomainNet dataset, due to the larger number of classes, we only demonstrate the results using semantics automatically acquired from LLMs, which are presented in

Table III. Given that Mini-DomainNet has a greater number of unseen classes, the difficulty of CDGZSL is also higher. The proposed MDASR achieves an H-accuracy ranging from 36.62% to 40.25% in different unseen domains, which remains the highest among all the methods compared. The results of the other methods are similar to those on Office-Home but with a general decline in H-accuracy. The domain shift problem effect is still severe with CDZSL methods. Under the CDZSL setting, their accuracy for unseen classes may reach 8.50%-25.90% [23], but under the CDGZSL setting, it’s only about 2%-5%. f-CLSWGAN still maintains a certain capacity for alleviating domain shift problem. If our MDASR is leveraged, the H-accuracy is further improved compared to f-CLSWGAN; however, if PCA is used for semantic refinement, since its objective function is to maximize variance, which is unrelated to the intrinsic semantics, it usually brings about a negative effect. Overall, in the two datasets, our proposed MDASR

TABLE IV  
THE ABLATION EXPERIMENT RESULTS ON MINI-DOMAINNET DATASET

	Clipart					Painting			Sketch		
	$\mathcal{L}_s$	$\mathcal{L}_{meta}$	S	U	H	S	U	H	S	U	H
Case (a):	✗	✗	61.38	24.53	35.05	58.23	23.31	33.29	56.60	22.03	31.71
Case (b):	✓	✗	61.34	29.32	39.67	58.29	20.23	30.03	57.32	26.02	35.79
Case (c):	✗	✓	63.73	26.15	37.08	59.98	23.82	34.10	55.41	26.25	35.62
Case (d):	✓	✓	63.69	29.43	40.25	61.02	26.16	36.62	55.16	28.25	37.36

achieved the highest H-accuracy, presenting the capacity to recognize seen and unseen classes in unseen domains.

Additionally, to further illustrate the effectiveness of the proposed MDASR in eliminating redundant semantics, we performed a two-dimensional visualization of the original semantic embeddings and the refined semantic embeddings, as shown in Fig. 7. Since the Mini-domainnet category count exceeds 100, considering spatial constraints and presentation effectiveness, we randomly selected 17 categories for display. From the figure, it can be seen that the refined semantics are more closely aligned with intrinsic visual features rather than other redundant information. For example, initially, in the original semantics, watermelon and broccoli are very close together but far from potato, which may suggest a large proportion of color in the original semantics since the first two are green. However, after refinement, the distance between watermelon and potato has decreased, indicating that the new semantics are no longer influenced by color, which can easily change with domain, but instead refer to the more difficult to alter 'shape,' as both are elliptically shaped. Furthermore, in the original semantics, vase and candle nearly overlap, which is inconsistent with visual features; the refined semantics also separate the two. Lastly, in the original semantics, butterfly, mosquito, and spider are far apart, but the refined semantics bring them closer together, which is also consistent with visual features. Overall, our method is effective in eliminating redundant components in semantics under the supervision of the common feature space.

#### D. Ablation Study

We conducted ablation experiments on the Mini-DomainNet dataset to prove the effectiveness of each component in our proposed method. The relevant results are presented in Table IV. There are a total of four sets of results, corresponding to whether similarity alignment loss  $\mathcal{L}_s$  and meta-learning loss  $\mathcal{L}_{meta}$  are used or not. Case (a) represents a generative method without any semantic refinement in the aligned space, and its results achieve 33.35% on average. Next, we verified the two parts of the proposed meta semantic refinement loss functions: the similarity matrix alignment  $\mathcal{L}_s$  and the meta-learning loss  $\mathcal{L}_{meta}$ . It can be observed that using only the similarity matrix alignment, as in case (b), some results improve while others worsen, suggesting that this method might lose certain important semantics. Solely utilizing meta-learning does not lead to degradation but offers limited improvement, as shown in case (c). Only by using both, as in case (d), do we

achieve the best semantic refinement results, which the average accuracy is 38.07%.

#### V. CONCLUSION

In this paper, we have introduced the task of cross-domain generalized zero-shot learning towards unseen domains for the first time and developed the MDASR approach which addresses the information asymmetry caused by the redundancy of LLM-based semantics. We construct a common feature space of seen domains, enabling the discriminative relations learned from the seen domains to generalize to unseen domains. Under the guidance of the common feature space, by designing ISA which aligns intra-class relationship, we have achieved the removal of non-intrinsic semantics. Meanwhile, through UMG that simulates the synthesis of unseen features, we retain intrinsic semantics that could connect the seen and unseen classes. Building on this, our proposed method can generate features of unseen classes by leveraging intrinsic semantics shared across domains, alleviating domain shift problem and recognizing both seen and unseen classes in unseen domains. We have validated the CDGZSL capabilities of our proposed method on two open-source datasets. On the Office-Home dataset, the average H-accuracy of CDGZSL reached 47.11%, and on the more challenging Mini-DomainNet dataset, the average H-accuracy of CDGZSL reached 38.07%. We have also made the corresponding semantics available to the public, providing a benchmark for future researchers.

#### REFERENCES

- [1] T. Brown, B. Mann, N. Ryder, M. Subbiah, J. D. Kaplan, P. Dhariwal, A. Neelakantan, P. Shyam, G. Sastry, A. Askell *et al.*, "Language models are few-shot learners," *Advances in neural information processing systems*, vol. 33, pp. 1877–1901, 2020.
- [2] W. X. Zhao and K. Zhou, "A survey of large language models," arXiv preprint arXiv: 2303.18223, 2023.
- [3] C. Chang, S. Wang, J. Zhang, J. Ge, and L. Li, "Llmscenario: Large language model driven scenario generation," *IEEE Transactions on Systems, Man, and Cybernetics: Systems*, 2024. doi: 10.1109/TSMC.2024.3392930.
- [4] J. Wang, P. Song, C. Zhao, and J. Ding, "Federated knowledge amalgamation with unbiased semantic attributes under cloud-edge collaboration for heterogeneous fault diagnosis," *Journal of Process Control*, vol. 131, p. 103095, 2023.
- [5] X. Wang, W. Huang, Y. Cheng, Q. Yu, and Z. Wei, "Multisource domain attribute adaptation based on adaptive multikernel alignment learning," *IEEE Transactions on Systems, Man, and Cybernetics: Systems*, vol. 50, no. 5, pp. 1897–1908, 2020.
- [6] B. Li and C. Zhao, "Federated zero-shot industrial fault diagnosis with cloud-shared semantic knowledge base," *IEEE Internet of Things Journal*, vol. 10, no. 13, pp. 11 619–11 630, 2023.

- [7] X. Wang, C. Chen, Y. Cheng, X. Chen, and Y. Liu, "Zero-shot learning based on deep weighted attribute prediction," *IEEE Transactions on Systems, Man, and Cybernetics: Systems*, vol. 50, no. 8, pp. 2948–2957, 2020.
- [8] L. Feng and C. Zhao, "Fault description based attribute transfer for zero-sample industrial fault diagnosis," *IEEE Transactions on Industrial Informatics*, vol. 17, no. 3, pp. 1852–1862, 2021.
- [9] C. H. Lampert, H. Nickisch, and S. Harmeling, "Attribute-based classification for zero-shot visual object categorization," *IEEE transactions on pattern analysis and machine intelligence*, vol. 36, no. 3, pp. 443–456, 2013.
- [10] X. Chen, B. Zhang, C. Zhao, J. Ding, and W. Wang, "From coarse to fine: Hierarchical zero-shot fault diagnosis with multigrained attributes," *IEEE Transactions on Fuzzy Systems*, vol. 32, no. 5, pp. 2837–2849, 2024.
- [11] Z. Akata, F. Perronnin, Z. Harchaoui, and C. Schmid, "Label-embedding for image classification," *IEEE transactions on pattern analysis and machine intelligence*, vol. 38, no. 7, pp. 1425–1438, 2015.
- [12] L. Feng, C. Zhao, and X. Li, "Bias-eliminated semantic refinement for any-shot learning," *IEEE Transactions on Image Processing*, vol. 31, pp. 2229–2244, 2022.
- [13] Y. Xian, T. Lorenz, B. Schiele, and Z. Akata, "Feature generating networks for zero-shot learning," in *Proceedings of the IEEE conference on computer vision and pattern recognition*, 2018, pp. 5542–5551.
- [14] X. Chen, J. Li, X. Lan, and N. Zheng, "Generalized zero-shot learning via multi-modal aggregated posterior aligning neural network," *IEEE Transactions on Multimedia*, vol. 24, pp. 177–187, 2022.
- [15] L. Feng and C. Zhao, "Transfer increment for generalized zero-shot learning," *IEEE Transactions on Neural Networks and Learning Systems*, vol. 32, no. 6, pp. 2506–2520, 2021.
- [16] Y. Ye, Y. He, T. Pan, J. Li, and H. T. Shen, "Alleviating domain shift via discriminative learning for generalized zero-shot learning," *IEEE Transactions on Multimedia*, vol. 24, pp. 1325–1337, 2022.
- [17] J. Yue, J. Zhao, and C. Zhao, "Similarity makes difference: SShTN for generalized zero-shot industrial fault diagnosis by leveraging auxiliary set," *IEEE Transactions on Industrial Informatics*, vol. 20, no. 5, pp. 7598–7607, 2024.
- [18] Y. Yang, X. Zhang, M. Yang, and C. Deng, "Adaptive bias-aware feature generation for generalized zero-shot learning," *IEEE Transactions on Multimedia*, vol. 25, pp. 280–290, 2023.
- [19] X. Sun, J. Gu, and H. Sun, "Research progress of zero-shot learning," *Applied Intelligence*, vol. 51, pp. 3600–3614, 2021.
- [20] M. F. Naeem, M. G. Z. A. Khan, Y. Xian, M. Z. Afzal, D. Stricker, L. Van Gool, and F. Tombari, "T2mvformer: Large language model generated multi-view document supervision for zero-shot image classification," in *Proceedings of the IEEE/CVF Conference on Computer Vision and Pattern Recognition*, 2023, pp. 15 169–15 179.
- [21] M. Mancini, Z. Akata, E. Ricci, and B. Caputo, "Towards recognizing unseen categories in unseen domains," in *European Conference on Computer Vision*. Springer, 2020, pp. 466–483.
- [22] H. Zhang, M. Cisse, Y. N. Dauphin, and D. Lopez-Paz, "Mixup: Beyond empirical risk minimization," in *International Conference on Learning Representations*, 2018.
- [23] B. Mondal and S. Biswas, "SEIC: Semantic embedding with intermediate classes for zero-shot domain generalization," in *Proceedings of the Asian Conference on Computer Vision*, 2022, pp. 789–806.
- [24] F. Pourpanah, M. Abdar, Y. Luo, X. Zhou, R. Wang, C. P. Lim, X.-Z. Wang, and Q. J. Wu, "A review of generalized zero-shot learning methods," *IEEE transactions on pattern analysis and machine intelligence*, vol. 45, no. 4, pp. 4051–4070, 2022.
- [25] Y. Ganin, E. Ustinova, H. Ajakan, P. Germain, H. Larochelle, F. Laviolette, M. Marchand, and V. Lempitsky, "Domain-adversarial training of neural networks," *The journal of machine learning research*, vol. 17, no. 1, pp. 2096–2030, 2016.
- [26] X. Cheng, Z. Rao, Y. Chen, and Q. Zhang, "Explaining knowledge distillation by quantifying the knowledge," in *Proceedings of the IEEE/CVF conference on computer vision and pattern recognition*, 2020, pp. 12 925–12 935.
- [27] N. Reimers and I. Gurevych, "Sentence-bert: Sentence embeddings using siamese bert-networks," in *Proceedings of the 2019 Conference on Empirical Methods in Natural Language Processing and the 9th International Joint Conference on Natural Language Processing (EMNLP-IJCNLP)*, 2019, pp. 3982–3992.
- [28] I. Gulrajani, F. Ahmed, M. Arjovsky, V. Dumoulin, and A. C. Courville, "Improved training of Wasserstein GANs," *Advances in neural information processing systems*, vol. 30, pp. 5769–5779, 2017.
- [29] H. Venkateswara, J. Eusebio, S. Chakraborty, and S. Panchanathan, "Deep hashing network for unsupervised domain adaptation," in *Proceedings of the IEEE Conference on Computer Vision and Pattern Recognition*, 2017, pp. 5018–5027.
- [30] K. Zhou, Y. Yang, Y. Qiao, and T. Xiang, "Domain adaptive ensemble learning," *IEEE Transactions on Image Processing*, vol. 30, pp. 8008–8018, 2021.
- [31] K. W. Church, "Word2Vec," *Natural Language Engineering*, vol. 23, no. 1, pp. 155–162, 2017.
- [32] J. Kocoń, I. Cichecki, O. Kaszyca, M. Kochanek, D. Szydło, J. Baran, J. Bielaniewicz, M. Gruza, A. Janz, K. Kanclerz *et al.*, "ChatGPT: Jack of all trades, master of none," *Information Fusion*, p. 101861, 2023.
- [33] X. Peng, Q. Bai, X. Xia, Z. Huang, K. Saenko, and B. Wang, "Moment matching for multi-source domain adaptation," in *Proceedings of the IEEE International Conference on Computer Vision*, 2019, pp. 1406–1415.
- [34] J. Deng, W. Dong, R. Socher, L.-J. Li, K. Li, and L. Fei-Fei, "Imagenet: A large-scale hierarchical image database," in *2009 IEEE conference on computer vision and pattern recognition*. IEEE, 2009, pp. 248–255.
- [35] S. Chandhok, S. Narayan, H. Cholakkal, R. M. Anwer, V. N. Balasubramanian, F. S. Khan, and L. Shao, "Structured latent embeddings for recognizing unseen classes in unseen domains," *arXiv preprint arXiv:2107.05622*, 2021.
- [36] V. Raunak, V. Gupta, and F. Metze, "Effective dimensionality reduction for word embeddings," in *Proceedings of the 4th Workshop on Representation Learning for NLP (RepL4NLP-2019)*, 2019, pp. 235–243.



**Jiaqi Yue** received the B.Eng. degree in automation from the College of Electrical Engineering, Zhejiang University, Hangzhou, China, in 2022, where he is currently pursuing the Ph.D. degree in control science and engineering with the College of Control Science and Engineering, Zhejiang University, Hangzhou, China. His current research interests include fault diagnosis and zero-shot learning.



**Jiancheng Zhao** received B.Eng. degree in automation from College of Control Science and Engineering, Zhejiang University, Hangzhou, China, in 2021, where he is currently pursuing the Ph.D. degree. His current research interests include industrial big data, zero-shot learning, few-shot learning.



**Chunhui Zhao** (SM'15) received Ph.D. degree from Northeastern University, China, in 2009. Since January 2012, she has been a Professor with the College of Control Science and Engineering, Zhejiang University, Hangzhou, China. Her research interests include statistical machine learning and data mining for industrial applications. She has authored or co-authored more than 140 papers in peer-reviewed international journals. She was the recipient of the National Top 100 Excellent Doctor Thesis Nomination Award, New Century Excellent Talents in University, China, and the National Science Fund for Excellent Young Scholars, respectively.